7

PHASE SPACE ANALYSIS OF NEURONAL EXCITABILITY

The previous chapter provided a detailed description of the currents underlying the generation and propagation of action potentials in the squid giant axon. The Hodgkin–Huxley (1952d) model captures these events in terms of the dynamical behavior of four variables: the membrane potential and three state variables determining the state of the fast sodium and the delayed potassium conductances. This quantitative, conductance-based formalism reproduces the physiological data remarkably well and has been extremely fertile in terms of providing a mathematical framework for modeling neuronal excitability throughout the animal kingdom (for the current state of the art, see McKenna, Davis, and Zornetzer, 1992; Bower and Beeman, 1998; Koch and Segev, 1998). Collectively, these models express the complex dynamical behaviors observed experimentally, including pulse generation and threshold behavior, adaptation, bursting, bistability, plateau potentials, hysteresis, and many more.

However, these models are difficult to construct and require detailed knowledge of the kinetics of the individual ionic currents. The large number of associated activation and inactivation functions and other parameters[1] usually obscures the contributions of particular features (e.g., the activation range of the sodium activation particle) toward the observed dynamic phenomena. Even after many years of experience in recording from neurons or modeling them, it is a dicey business predicting the effect that varying one parameter, say, the amplitude of the calcium-dependent slow potassium current (Chap. 9), has on the overall behavior of the model. This precludes the development of insight and intuition, since the numerical complexity of these models prevents one from understanding which important features in the model are responsible for a particular phenomenon and which are irrelevant.

Qualitative models of neuronal excitability, capturing some of the *topological aspects* of neuronal dynamics but at a much reduced complexity, can be very helpful in this regard, since they highlight the crucial features responsible for a particular behavior. By topological

1. The electrical model of the spiking behavior of the bullfrog sympathetic ganglion cells, illustrated in Figs. 9.10–9.12, includes eight ionic currents, which are described with the help of two dozen voltage and/or calcium-dependent functions and an equal number of additional parameters. And this is for a spherical neuron devoid of any dendrites.

aspects we mean those properties that remain unchanged in spite of quantitative changes in the underlying system. These typically include the existence of stable solutions and their basins of attraction, limit cycles, bistability, and the existence of strange attractors. In this chapter we discuss two-dimensional models of spiking systems, a qualitative as well as quantitative, biophysical model, that will help us to understand a number of important features of the Hodgkin–Huxley (and related) membrane patch models using the theory of dynamical systems and phase space analysis. In particular, the FitzHugh–Nagumo model explains the origin and onset of neuronal oscillations, that is, periodic spike trains, in response to a sustained current input. It is considerably easier—from both a numerical and a conceptual point of view—to study the dynamics of populations of neuronal "units" described by such simplified dynamics rather than simulating the behavior of a network of biophysically complex neurons.

For a general introduction to the theory of dynamical systems, see the classical treatise of Hirsch and Smale (1974) or the informal and very friendly account by Strogatz (1994) that stresses applications. Two eminently readable introductions to physiological applications of this theory are the monograph by Glass and Mackey (1988) and the chapter by Rinzel and Ermentrout (1998).

Following the ancient wisdom that "there's no such thing as a free lunch," we can well ask what is the price that one pays for this elegance? The answer is that simple models usually lack numerically accurate predictions. As we will see below, we can understand why oscillations in one system will be initiated with a nonzero firing frequency, as in the squid giant axon, while other systems, such as neocortical pyramidal cells, can respond with a train of spikes having very long interspike intervals. Yet, in general, these models do not allow precise predictions to be made concerning the exact threshold for the onset of spikes and so on. This drawback is less serious than in other fields of science, however, since in almost all situations of interest, precise knowledge of the relevant biophysical parameters is lacking anyway. Given the fantastic diversity and variability among neurons, simple generic models are frequently much superior at capturing key aspects of neuronal function, in particular at the network level, than detailed ones.

7.1 The FitzHugh–Nagumo Model

The simplified model of spiking is justified by the observation that in the Hodgkin–Huxley equations, both the membrane potential $V(t)$ as well as the sodium activation $m(t)$ evolve on similar time scales during an action potential, while sodium inactivation $h(t)$ and potassium activation $n(t)$ change on similar, albeit much slower time scales. This can be visualized by plotting V and m, representing the "excitability" of the system, using normalized coordinates in response to a current step (Fig. 7.1A). Given the great similarity between both variables, it makes sense to lump them into a single "activation" variable V (Fig. 7.1C). The same observation can be made if one plots the degree of potassium activation n together with the amount of sodium inactivation $1 - h$ for the identical current stimulus (Fig. 7.1B). Again, because both variables show the same changes of almost the same amplitude over time, we combine both into a single variable W, characterizing the degree of "accommodation" or "refractoriness" of the system (Fig. 7.1D). The behavior of such a two-dimensional system with constant parameters is qualitatively very similar to the behavior of the four-dimensional Hodgkin–Huxley model with voltage-dependent functions $m_\infty(V)$, $\tau_m(V)$ and so on.

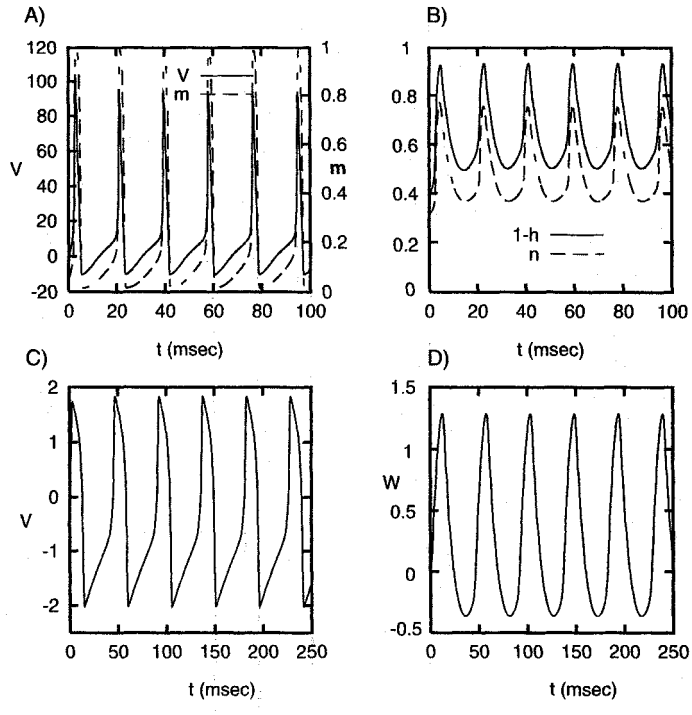

Fig. 7.1 Reducing the Hodgkin–Huxley Model to the FitzHugh–Nagumo System Evolution of the space-clamped Hodgkin–Huxley and the FitzHugh-Nagumo equations in response to a current step of amplitude 0.18 nA in A and B and of amplitude I = 0.35 in C and D. **(A)** Membrane potential $V(t)$ and sodium activation $m(t)$ (see also Fig. 6.8). Sodium activation closely follows the dynamics of the membrane potential. **(B)** Sodium inactivation $1 - h$ and potassium activation n of the Hodgkin–Huxley system. **(C)** "Excitability" $V(t)$ of the two-dimensional FitzHugh–Nagumo equations (Eqs. 7.1) with constant parameters has a very similar time course to V and m of the squid axon (notice the different scaling). **(D)** The "accommodation" variable W shows modulations similar to $1 - h$ and n of the Hodgkin–Huxley equations.

We will let Fig. 7.1 (and others to follow) be sufficient justification for this reduction. We refer those of our readers who are not satisfied by the somewhat *ad hoc* nature of this procedure to Kepler, Abbott, and Marder (1992), who describe a general method for reducing Hodgkin-Huxley-like systems using "equivalent potentials."

Historically, the equations underlying the FitzHugh–Nagumo model have their origin in the work of van der Pol (1926), who formulated a nonlinear oscillator model (termed a relaxation oscillator) and applied it to the cardiac pacemaker (van der Pol and van der Mark, 1928). Using the phase space method explored by Bonhoeffer (1948) in the context of a chemical reaction bearing some similarities to nerve cell excitation, FitzHugh (1961, 1969) and, independently, Nagumo, Arimoto, and Yoshizawa (1962) derived the following two equations to qualitatively describe the events occurring in an excitable neuron:

$$\dot{V} = V - \frac{V^3}{3} - W + I$$

$$\dot{W} = \phi(V + a - bW) \tag{7.1}$$

where we use the conventional shorthand of writing $\dot{V}$ for the temporal derivative of

V, dV/dt. Equations 7.1 describe the so-called *FitzHugh–Nagumo* model or, in deference to earlier work by van der Pol (1926) and Bonhoeffer (1948), the *Bonhoeffer–van der Pol* model. The parameters a, b, and ϕ are dimensionless and positive, with a number of different versions of these equations in usage. In this chapter, we assume $a = 0.7$, $b = 0.8$, and $\phi = 0.08$ (Cronin, 1987). The amplitude of ϕ, corresponding to the inverse of a time constant, determines how fast the variable W changes relative to V. With $\phi = 0.08$, V changes substantially more rapidly than W (since $\dot{V}$ is typically $1/0.08 = 12.5$ times larger than $\dot{W}$).

Equations 7.1 represent an instance of a *singularly perturbed system*, where one variable (or set of variables) evolves much faster than the other variable (or set of variables). This has the consequence that the evolution of the system consists of "rapid" segments, in which the fast variable V evolves so rapidly that the slow variable W can be considered stationary, interconnected with "slow" segments, during which the slow variable will not remain constant, as during the fast segments, but will be an instantaneous function of the fast variable $W = W(V(t))$ (for more details, see Cronin, 1987).

Because of the nonlinear nature of these differential equations, closed-form solutions are difficult to derive and we are forced to integrate the equations numerically. We can, however, deduce the qualitative topological properties of these equations *without* explicitly solving them. The key concept here is to consider the evolution of the system, specified by the vector $r(t) = (V(t), W(t))$, in the associated two-dimensional *phase space*, spanned by V and W (Fig. 7.2). For every state or phase point $\mathbf{r}$ in this plane, Eqs. 7.1 assign a vector $\dot{\mathbf{r}} = (\dot{V}, \dot{W})$ to this point, specifying how the system will evolve in time. Indeed, these equations can be thought of as a vector field in phase space, akin to the motion of an imaginary laminar fluid on the plane. While only a few representative vectors are drawn in Fig. 7.2, they completely fill the plane. Such plots are known as *phase plane portraits* and provide an intuitive and geometrical way to understand certain qualitative aspects of the solution of the associated ordinary differential equations.

In cases such as Eqs. 7.1, where the derivatives on the right-hand side do not depend explicitly on time, different trajectories can never cross, since if two would intersect, there would be two different solutions starting from the same (crossing) point. This is ruled out by the existence and uniqueness theorem associated with a set of coupled differential equations, such as these, that are smooth enough. Thus, from any point in the phase space, the system can only evolve in one way, giving phase portraits their orderly looks.

7.1.1 Nullclines

In order to understand how the system evolves in time, let us consider two of its isoclines. An *isocline* is a curve in the (V, W) plane along which one of the derivatives is constant. In particular, the null isocline, or *nullcline*, is the curve along which either $\dot{V}$ or $\dot{W}$ is zero. The nullcline associated with the fast variable V, defined by $\dot{V} = 0$, is the cubic function $W = V - V^3/3 + I$. If the system currently is located on the V nullcline, its imminent future trajectory must be vertical, pointing either upward (for $\dot{W} > 0$) or downward (for $\dot{W} < 0$). Furthermore, for all points in the plane above this cubic polynomial, $\dot{V} < 0$, while the converse is true for all points below the curve $W = V - V^3/3 + I$.

The nullcline associated with the slow variable, $\dot{W} = 0$, is specified by the linear equation $W = (V + a)/b$. Thus, if the evolution of the system brings it onto the W nullcline, its trajectory in the immediate future must be horizontal, for only V, but not W, can change. Furthermore, all phase points in the half-plane to the left of $W = (V + a)/b$ have a

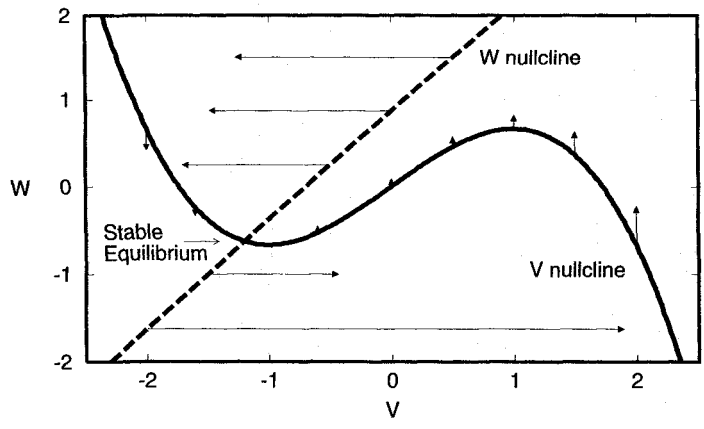

Fig. 7.2 PHASE PLANE PORTRAIT OF THE FITZHUGH–NAGUMO MODEL Phase plane associated with the FitzHugh–Nagumo Eqs. 7.1 for $I = 0$. The fast variable V corresponds to membrane excitability while the slower variable W can be visualized as the state of membrane accommodation. The nullcline for the V variable, that is, all points with $\dot{V} = 0$, is a cubic polynomial, and the W nullcline (all points with $\dot{W} = 0$) is a straight line. The system can only exist in equilibrium at the intersection of these curves. For our choice of parameters and for $I = 0$, a single equilibrium point exists: $(\overline{V}, \overline{W}) = (-1.20, -0.625)$. The arrows are proportional to $(\dot{V}, \dot{W})$ and indicate the direction and rate of change of the system: V usually changes much more rapidly than W.

negative W derivative and therefore move downward, while points in the right half-plane are associated with increasing W values.

As mentioned above, the FitzHugh–Nagumo equations are an example of an *autonomous* system whose derivatives do not explicitly depend on time (assuming that I has some constant value for $t \geq 0$). If the right-hand side of Eqs. 7.1 would contain terms that explicitly depended on time t (such as a time-dependent forcing term $I(t)$), the nullclines would change with time. The trajectory $(V(t), W(t))$ of the system in phase space can now cross itself and our simple analysis no longer applies.

7.1.2 Stability of the Equilibrium Points

Let us first analyze the resting states of the system and their stability. The *fixed, critical,* or *singular points* of the system r^* are all those points (V_i, W_i) at which both derivatives are zero, that is, for which $(\dot{V}(V_i, W_i), \dot{W}(V_i, W_i)) = (0, 0)$. For Eqs. 7.1 with our choice of parameter values and $I = 0$, the two nullclines meet at a single point $\mathbf{r}^* = (\overline{V}, \overline{W}) = (-1.20, -0.625)$. If the system started out exactly at this point, it would not move to any other point in phase space. This is why it is known as an equilibrium point. However, in the real world, the system will never be precisely at the critical point but in some neighborhood around this point. Or, if the system started exactly at the critical point $(\overline{V}, \overline{W})$, any noise would perturb it and carry it to a point in the immediate neighborhood $(\overline{V} + \delta V, \overline{W} + \delta W)$. The subsequent fate of the perturbed system depends on whether the fixed point is stable or not. In the former case, the system will eventually return to $(\overline{V}, \overline{W})$. If the equilibrium point is not stable, the system will diverge away from the singular point.

The stability of the equilibrium point can be evaluated by linearizing the system around the singular point and computing its eigenvalues. Conceptually, this can be thought of as zooming into the immediate neighborhood of this point. The linearization procedure

corresponds to moving the origin of the coordinate system to the singular point and considering the fate of points in the immediate neighborhood of the origin (Fig. 7.3A). The associated eigenvalues of the linear system completely characterize the behavior in this neighborhood. Following Eqs. 7.1, we can write for any perturbation δ **r** around the fixed point **r***,

$$\dot{\overline{V}} + \delta\dot{V} = (\overline{V} + \delta V) - (\overline{V} + \delta V)^3/3 - (\overline{W} + \delta W) + I$$

$$\dot{\overline{W}} + \delta\dot{W} = \phi((\overline{V} + \delta V) + a - b(\overline{W} + \delta W)) \tag{7.2}$$

Remembering that $(\overline{V} - \overline{V}^3/3 - \overline{W} + I) = 0$ and $\phi(\overline{V} + a - b\overline{W}) = 0$ (the definition of the critical point) as well as $\dot{\overline{V}} = \dot{\overline{W}} = 0$ and neglecting higher order terms in δV (since the perturbation is assumed to be small), we arrive at

$$\delta\dot{V} = (1 - \overline{V}^2)\delta V - \delta W$$

$$\delta\dot{W} = \phi(\delta V - b\delta W) \tag{7.3}$$

or, in obvious vector notation,

$$\delta\dot{\mathbf{r}} = M\delta\mathbf{r} \tag{7.4}$$

with the matrix M given by

$$M = \begin{bmatrix} (1 - \overline{V}^2) & -1 \\ \phi & -b\phi \end{bmatrix} \tag{7.5}$$

This corresponds to the matrix of partial derivatives associated with Eqs. 7.1 and evaluated at the critical point.

Equation 7.4 describes how any perturbation δ**r** evolves in the neighborhood of the singular point **r***. We can characterize the behavior around this point by finding the eigenvalues of M. The associated characteristic equation is

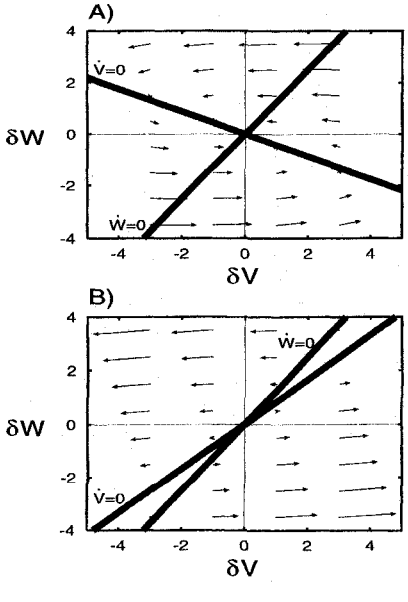

Fig. 7.3 Behavior around the Equilibrium Point The behavior of the FitzHugh–Nagumo equations in a small neighborhood around the fixed point is determined by linearizing these equations around their fixed point and computing the associated pair of eigenvalues. **(A)** Evolution of $(\delta V, \delta W)$ in a coordinate system centered at the equilibrium point **r*** for $I = 0$. Because the real part of both eigenvalues is negative, a small perturbation away from the fixed point will decay to zero, rendering this point asymptotically stable. Any point in this plane will ultimately converge to the fixed point at the origin. **(B)** Similar analysis for the equilibrium point **r***′ for a sustained input with $I = 1$ (Fig. 7.5A). The fixed point is unstable.

$$\lambda^2 + (\overline{V}^2 - 1 + b\phi)\lambda + (\overline{V}^2 - 1)b\phi + \phi = 0\,. \tag{7.6}$$

The eigenvalues correspond to the solutions of this equation,

$$\lambda_{1,2} = \frac{-(\overline{V}^2 - 1 + b\phi) \pm \sqrt{(\overline{V}^2 - 1 - b\phi)^2 - 4\phi}}{2}\,. \tag{7.7}$$

The evolution of the system therefore takes the following form:

$$\delta\mathbf{r}(t) = c_1\mathbf{r}_1 e^{\lambda_1 t} + c_2\mathbf{r}_2 e^{\lambda_2 t} \tag{7.8}$$

with $\mathbf{r}_1$ and $\mathbf{r}_2$ the two eigenvectors associated with the eigenvalues λ_1 and λ_2 and c_1 and c_2 depending on the initial conditions of the system.

In the two-dimensional case considered here, the different types of solutions of Eqs. 7.1 are easy to classify and understand geometrically in terms of the eigenvalues. In order to study the ultimate fate of the fixed points, the exact values of λ_1 and λ_2 do not matter. What does matter is whether or not the eigenvalues are real or imaginary and the sign of their real parts. (For a thorough discussion of this see Hirsch and Smale, 1974, and Strogatz, 1994.)

1. If λ_1 and λ_2 are both real and at least one of them is positive, the perturbation $\delta r(t)$ will grow without bounds and the solution will diverge from the fixed point: the critical point is unstable. If both eigenvalues are positive, the point is called a *source*; if one of them is positive and the other negative, the point is called a *saddle*.

2. When the eigenvalues are real and both negative, $\delta\mathbf{r}(t) \to 0$ and the system will decay back to its resting state: the critical point is stable and termed a *sink*.

3. If the expression under the square root in Eq. 7.7 becomes negative, the two eigenvalues form a complex conjugate pair with $\lambda_1 = \alpha + i\omega$ and $\lambda_2 = \alpha - i\omega$, and we have

$$\delta\mathbf{r}(t) = c_1\mathbf{r}_1 e^{\alpha t} e^{i\omega t} + c_2\mathbf{r}_2 e^{\alpha t} e^{-i\omega t}\,. \tag{7.9}$$

   Note that the eigenvectors $\mathbf{r}$ are complex, since the λ's are. Exploiting Euler's formula, $e^{i\omega t} = \cos\omega t + i\sin\omega t$, we can reexpress the evolution of the perturbation as a combination of terms involving $e^{\alpha t}\cos(\omega t)$ and $e^{\alpha t}\sin(\omega t)$.

   This evolution equation has two parts; the first one, $e^{\alpha t}$, specifies whether the system will converge back to its resting state or whether it will diverge, depending on the sign of α, that is, on the sign of the real part of the eigenvalues. The second part can be thought of as a rotation around the origin, with the oscillation frequency given by $f = \omega/(2\pi)$. For $\omega > 0$, the trajectories will be traversed counterclockwise and clockwise if $\omega < 0$. If $\alpha = 0$, the system will always remain at a fixed distance from the center and will neither approach nor recede from this periodic trajectory. For $\alpha < 0$, the system will display damped oscillations and converge toward the equilibrium state. Here, the fixed point $(\overline{V}, \overline{W})$ is termed a stable *spiral* or *attractor*. Conversely, if $\alpha > 0$, the oscillations will grow exponentially in amplitude and the equilibrium point is an *unstable spiral* or focus.

Returning to the FitzHugh–Nagumo model in the case of no current input, the two eigenvalues associated with the equilibrium point at rest ($I = 0$) are $-0.50 \pm 0.42i$. According to our argumentation, this implies that any perturbation $\delta\mathbf{r}$ decays in an exponential manner back to zero, that is, back to the equilibrium point, since the real part of the eigenvalues is

negative (see Fig. 7.3A). Because the solution will also oscillate, the equilibrium point is a stable spiral or attractor.

How large is the neighborhood around the equilibrium point within which any perturbation will ultimately die out? The size of the largest such neighborhood is called the *basin of attraction* associated with this stable point, that is, the set of initial conditions $\mathbf{r}_0 = (V_0, W_0)$ in phase space that will ultimately "fall into" this stable point. In our case, the basin is the entire plane. In other words, no matter what the initial conditions, in the absence of any stimulus current I the system will ultimately always come to rest at $\mathbf{r}^*$.

This illustrates the power of phase space analysis. The stability of any nonlinear autonomous system of differential equations can be analyzed in terms of the stability of the linearized system; the signs of the real part of the eigenvalues then determine the qualitative behavior of the system in some neighborhood around the equilibrium point (Hirsch and Smale, 1974). By looking for the intersections of the nullclines when changing the differential equations characterizing the system, one can immediately understand in an intuitive manner the steady-state properties of the system (see Strogatz, 1994, for many biologically inspired examples of this).

7.1.3 Instantaneous Current Pulses: Action Potentials

How will the FitzHugh–Nagumo model respond if an instantaneous current pulse $I(t) = Q\delta(t)$ (with $Q > 0$) is applied? The initial value of V will jump by Q, thereby moving the system in phase space a certain horizontal distance away from the equilibrium point (dashed line in Fig. 7.4A). The direction of the movement is determined by the sign of the current input.

If the amplitude of the current input is small, the system will almost immediately return to rest following a tight trajectory around the equilibrium point. In the process, V will over- and undershoot the resting state $\overline{V} = -1.2$ (since the eigenvalues are complex), typical of a system with an inductance-like behavior (see Chap. 10). However, in order to see these oscillations around $\mathbf{r}^*$, Fig. 7.4B would have to be enlarged. The trajectory of V reminds us of the subthreshold response of the Hodgkin–Huxley membrane model (Fig. 6.5B). There, a short current pulse also depolarizes the membrane, activating some potassium current and slightly hyperpolarizing the membrane, before finally settling down at the resting potential. Both in the Hodgkin–Huxley and in the FitzHugh–Nagumo systems, graded "potentials" can be obtained by varying the amplitude of the initial displacement over a small range of values.

What happens if the amplitude of the current pulse is made larger? If V is moved instantaneously past -0.64, the evolution of the system sharply veers away from the V nullcline, with V rapidly increasing while W remains more or less stationary until the rightmost branch of the V nullcline is encountered, defining the maximal value of V. The reason for this rapid change is that $\dot{V}$ is large, while $\dot{W}$, due to the small size of ϕ, is small (the slope dW/dV of the trajectory is on the order of ϕ; Eqs. 7.1). During the next phase, the system slowly "crawls" upward along the V nullcline until it reaches the knee at the top of this curve. This slow phase is dictated by the fact that $\dot{V}$ is very small in the neighborhood of this curve, causing W to be an instantaneous function of V (the slope of the trajectory dW/dV is large here). A third "fast" phase follows, where V is rapidly reduced, undershooting the resting value of $\overline{V}$ in the process. Finally, the system slowly loses its accommodation W, crawling back to the resting state along the left branch of the nullcline. This trajectory is very much reminiscent of a Hodgkin–Huxley action potential

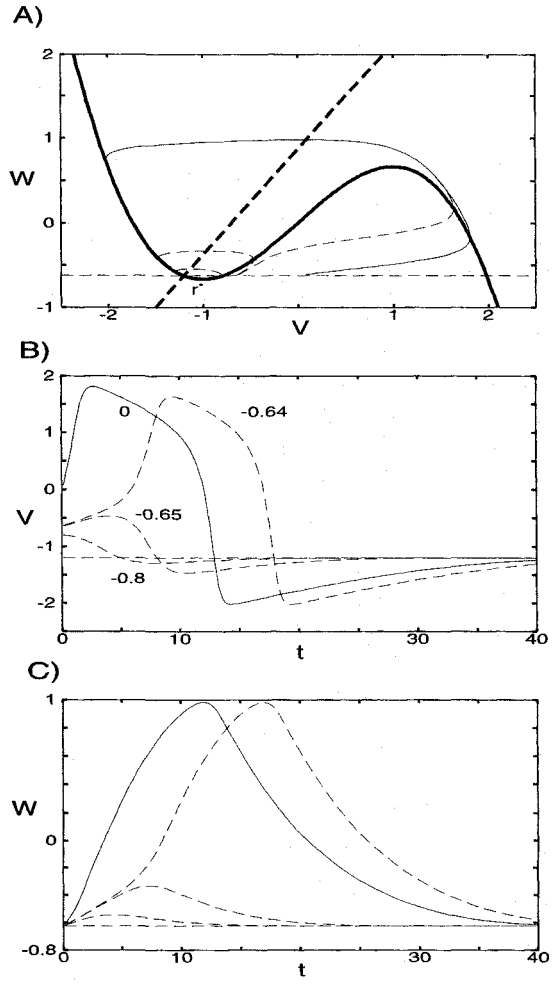

Fig. 7.4 Response of the FitzHugh–Nagumo Model to Current Pulses **(A)** The quiescent system is excited by a current pulse of different amplitudes $I = Q\delta(t)$, displacing the system from its resting state $\mathbf{r}^*$ along the dashed horizontal line. Following Eqs. 7.1, this briefly increases $\dot{V}$, in agreement with physical intuition, since a brief current pulse will cause a transient capacitive current $C\,dV/dt$ to flow. The evolution of the voltage V and of the adaptation variable W is plotted in **(B)** and **(C)**. Changing V from its initial value of -1.2 to -0.8 or -0.65 only causes quick excursions of the voltage around the equilibrium point with the system rapidly returning to rest (the oscillatory manner in which the system does so is not readily apparent at the scale of these panels). If the current pulse is large enough so that V exceeds -0.64, a stereotyped "all-or-none" sequence is triggered: V rapidly increases to positive values but then dives below its resting value $\overline{V}$ before finally coming to rest again at $\mathbf{r}^*$. Notice that the trajectory in this case consists of "fast" segments, where V changes rapidly but W remains essentially constant (upper and lower segments), interconnected by "slow" segments, where the system changes so slowly that V is always in equilibrium (the "slow" segments closely coincide with the V nullcline).

(Fig. 6.5), with V and sodium activation m changing rapidly, while sodium inactivation h and potassium activation n vary at a more leisurely pace.

While the system is "hyperpolarized," that is, traveling along the leftmost branch of the V nullcline, it is clear that the inactivation variable W must be brought down below its

resting value of about -0.625 before the system can cross over the W nullcline and once again execute its standard trajectory. This is equivalent to a *refractory* period, during which much larger current pulses are needed in order to trigger another spike.

As emphasized above, this behavior, with "fast" segments along which accommodation varies little but V changes rapidly, connected by "slower" segments where V is in equilibrium as W changes slowly, is typical of singularly perturbed systems (Cronin, 1987). Injecting larger current pulses will not change this basic trajectory, even though each value of I is associated with its own unique trajectory in phase space.

Although we stated above that the system goes through its stereotypical trajectory once V exceeds -0.64, the FitzHugh–Nagumo system shows no true threshold behavior. From a numerical point of view, the amplitude Q of the current pulse can be varied by minute amounts between -0.65 and -0.64, giving rise to all possible intermediate trajectories between sub- and suprathreshold (filling in the available phase space between the two associated trajectories in Fig. 7.4A). Indeed, it is known both computationally (Cooley and Dodge, 1966) and experimentally (at higher temperature; Cole, Guttman, and Bezanilla, 1970) that the squid action potential does not behave in a true all-or-none manner. In both systems, no true *saddle* exists in the sense that all points to one side of the saddle will remain below and all points beyond the saddle will be above threshold. However, if ϕ is small, points close to the middle part of the V nullcline act approximately as a *separatrix*, from which neighboring paths diverge sharply to the left or to the right. The "width" of the separatrix over which intermediate forms between sub- and suprathreshold responses exist is so small that from a physiological point of view (given the ambient level of variability in the membrane potential), the system does show threshold behavior, with the horizontal distance between the resting point and the separatrix corresponding to the amplitude of the threshold.

7.1.4 Sustained Current Injection: A Limit Cycle Appears

Let us stimulate the quiescent system with a sustained current step of amplitude I at $t = 0$. This input will, different from a current pulse, change the associated phase space diagram. We can visualize the new phase diagram by noticing that for a positive current step the V nullcline is shifted upward, while the W nullcline does not change (Fig. 7.5A). This, of course, changes the position of the equilibrium point. In the presence of a positive current up to three fixed points now coexist, since the cubic V nullcline can intersect the linear W nullcline at up to three different locations. However, both geometrical intuition (the slope of the W nullcline is too steep to intersect the V nullcline more than once) as well as an algebraic criterion (Cardan's solution) tell us that for $b < 1$ only a single solution exists. The solution is stable as long as the real part of the two eigenvalues is negative. Once the real part becomes zero and then positive, even infinitesimal small perturbations will become amplified and diverge away from the equilibrium point. Following Eq. 7.7, the real part changes sign at the two locations where

$$\overline{V}_{\pm} = \pm\sqrt{1 - b\phi}\,. \tag{7.10}$$

Thus, the equilibrium point is stable whenever the W nullcline meets the cubic nullcline along its right- and leftmost branches. Here the slope is negative and $|\overline{V}| \geq 1$. However, along the central part of the V nullcline, $|\overline{V}| < \sqrt{1 - b\phi}$, and the eigenvalues will acquire a positive real part, rendering the fixed point unstable.

Assuming that the system is in its quiescent state $\mathbf{r}^* = (\overline{V}, \overline{W}) = (-1.20, -0.625)$, then as long as the amplitude of the current step is small enough, the real part of the

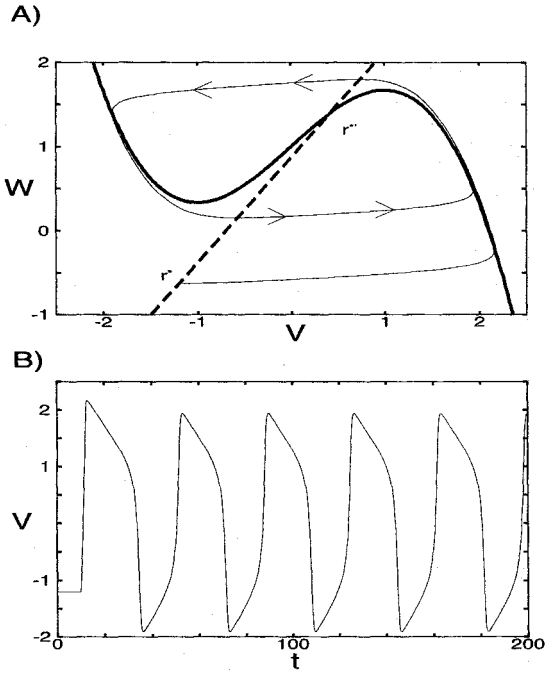

Fig. 7.5 Response of the Fitz-Hugh–Nagumo Model to Current Steps (**A**) The quiescent system is subject to a current step of amplitude I. For $I < 0.32$, the new equilibrium $\mathbf{r}^{*\prime}$ is stable: the system depolarizes but remains subthreshold. For larger steps (here $I = 1$), the new equilibrium point lies along the middle portion of the V nullcline and is unstable. Because the system has a stable limit cycle, it will not diverge; rather, it generates a train of "action potentials" whose time course is shown in (**B**). Regardless of the initial state of the system, it will always converge rapidly onto this limit cycle.

eigenvalues associated with the new equilibrium point $\mathbf{r}^{*\prime}$ remains negative and $\mathbf{r}^{*\prime}$ is stable. Because of the upward shift of the V nullcline, the new resting state of the membrane potential $\overline{V}'$ is more positive than $\overline{V}$, that is, the system is depolarized.

For a critical value of the input current I_{-}, the nullclines intersect along the central part of the V nullcline at $\overline{V}_{-}$ (defined by Eq. 7.10) and local stability breaks down (as in Fig. 7.5B). Due to the cubic nonlinearity in Eqs. 7.1, the system does not diverge[2] but follows a stereotypical trajectory around $\mathbf{r}^{*\prime}$. As demonstrated in Fig. 7.5, the system moves from its starting point rapidly to the right ("the membrane depolarizes") until it meets the rightmost branch of the V nullcline where it will slowly creep upward (adaptation builds up). Subsequently, V decays rapidly by moving horizontally toward the right and down the leftmost branch of the V nullcline. So far, the behavior of the equations is very similar to that seen earlier, with fast phases alternating with phases during which the system crawls along the V nullclines (the arrows in Fig. 7.2 give a good feeling for the relative speed of these processes).

Different from before, the system does not return to its new equilibrium point $\mathbf{r}^{*\prime}$, since this is unstable. Rather the trajectory of the system undershoots $\mathbf{r}^{*\prime}$ and traces a path almost parallel to the V axis until it meets its previous trajectory, which it then follows. As long as the input I_0 persists, the system continues to evolve along the same trajectory, producing a constant and infinite stream of action potentials (Figs. 7.1C and 7.5B). Since these oscillations are stable, but the term "steady-state" usually refers to an unchanging and not to a changing state, another label is needed. The French mathematician Poincaré, to whom we owe phase space analysis of differential equations with two variables, called such steady oscillations a *stable limit cycle*.

2. As it would in a purely linear system once the system looses stability.

If the system starts out at a location in phase space inside the limit cycle, its trajectory will spiral outward until it meets the limit cycle. Likewise, for any point outside the limit cycle, the system will spiral into the limit cycle. Thus, the *basin of attraction* of the limit cycle is the entire phase plane (with the exception of the equilibrium point). The limit cycle is stable, since small perturbations away from the cycle will be quickly suppressed and the system will return to the limit cycle. In order for a closed, that is, oscillatory, solution to be a limit cycle is must have an *isolated trajectory*. This implies that any neighboring trajectories must either spiral toward (as they do here) or away from the limit cycle (unstable limit cycle). This is where the sense of the word "limit" in limit cycles comes from.

Limit cycles are inherently nonlinear phenomena; they cannot occur in a linear system. Obviously, linear systems can oscillate, as shown by the harmonic oscillator, that is they have closed orbits. Yet these trajectories are not isolated. If $\mathbf{r}(t)$ is an oscillatory solution, so will $c\mathbf{r}(t)$, for any value of c. For such a system, the initial conditions will always dictate the exact orbit chosen by the system. The system never forgets this, no matter how long one waits. This is quite distinct from a limit cycle in a nonlinear system, such as the Hodgkin–Huxley or the FitzHugh-Nagumo equations, where, given a strong enough input, the system will ultimately converge to the limit cycle. The cubic nonlinearity in Eqs. 7.1 is essential for the overall behavior of the system.

Limit cycles cannot exist in systems with only one degree of freedom that are governed by a first-order differential equation, no matter whether linear or nonlinear. Such systems either converge toward their fixed points or they diverge to infinity. No overshooting or damped oscillations can occur.

7.1.5 Onset of Nonzero Frequency Oscillations: The Hopf Bifurcation

What governs the onset of oscillations? Is it possible to obtain spiking with arbitrarily low frequencies? The coupled nonlinear differential equations that arise within a biophysical context can display two fundamentally different types of onset of oscillations, one related to a *Hopf bifurcation* and one related to the creation of a *saddle*. Both behave in very different ways, which are of functional relevance. We will study the first type of bifurcation here, deferring the second one to the following section.

As discussed in the previous section, increasing the amplitude of the injected current I from zero to more positive values shifts the intersection of the two nullclines (Fig. 7.5). As I increases, so does the real part α of the eigenvalue associated with the equilibrium point at its resting value. Breakdown of stability occurs when α changes sign, since for $\alpha > 0$, small perturbations in the neighborhood of the equilibrium point will fail to die out. Based on Eq. 7.7, $\alpha = 0$ occurs if and only if $\overline{V} = \pm\sqrt{1 - b\phi}$. These two voltages are associated with two different values of the input current, $I_- = 0.33$ and $I_+ = 1.42$.

At these two values of the input current, the equilibrium point ceases to be stable and develops into an unstable source. The system starts to oscillate, with a frequency determined by the imaginary part of the associated eigenvalues (Fig. 7.6B). Whether or not these oscillations develop into a stable limit cycle, as here or as in the case of the Hodgkin–Huxley equations, depends on the global character of the equations and cannot be determined based on a local criterion.

This type of dynamical phenomenon, in which stable large-amplitude oscillations arise abruptly as one particular parameter, known as the *bifurcation parameter* (here I), varies smoothly, is called *hard excitation*, or *subcritical Hopf bifurcation*. Hard excitation is feared in engineering applications, since one of its salient properties is that the amplitudes of the

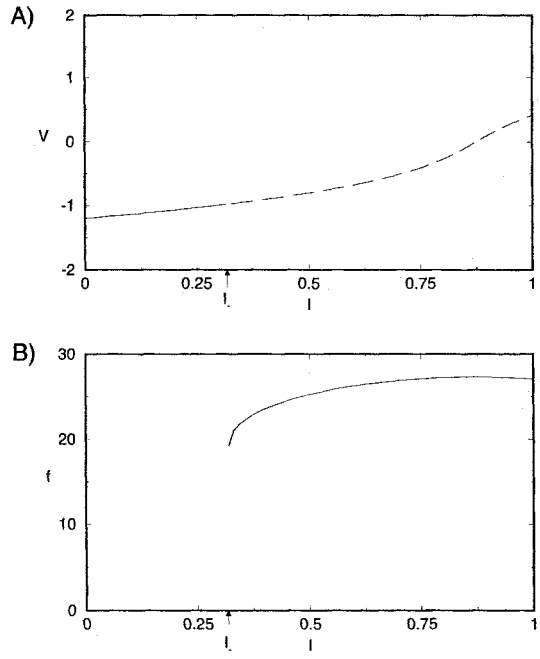

Fig. 7.6 DISCHARGE CURVE OF THE FITZHUGH–NAGUMO MODEL **(A)** Steady-state membrane potential and **(B)** oscillation frequency of the limit cycle for the FitzHugh–Nagumo equations as a function of a sustained current I. As the membrane is depolarized in response to increasing injection of current, it loses stability at $I_- = 0.33$ (arrow) and moves on a stable limit cycle. An important property of this type of bifurcation phenomenon, known as hard excitation or subcritical Hopf bifurcation, is that oscillations occur with nonzero frequency. This behavior is also characteristic for the Hodgkin–Huxley equations. Between I_- and $I_+ = 1.42$, the system moves along the limit cycle. The frequency of the oscillation is a function of I (dashed line in panel A). Beyond I_+, the equilibrium point becomes stable again, and the system remains "locked" at a depolarized level (not shown).

oscillations are nonzero and can be fairly large. A *soft excitation*—also known as *supercritical Hopf bifurcation*—occurs when oscillations arise with arbitrarily small amplitudes and gradually increase as the bifurcation parameter is ramped up. Hard excitation constitutes one of the generic mechanisms for the onset of oscillations in coupled nonlinear differential equations (Glass and Mackey, 1988; Strogatz, 1994). A subcritical Hopf bifurcation requires that a stable spiral or attractor change into an unstable spiral and is surrounded by a stable limit cycle.

A key feature of a Hopf bifurcation is the onset of a stable limit cycle with a nonzero oscillation frequency (since ω is finite). It is a well-known feature of the Hodgkin–Huxley model that the minimal stable spiking frequency is about 50 Hz (at 6.3°; see Fig. 6.9B). Experimentally, this is true for most axonal membranes as well as for the generation of spike trains at the cell body of certain neuronal types, for instance, the nonadapting cortical interneurons. As we keep on increasing I, the frequency of these stable oscillations first increases before the f–I curve peaks and decreases back to 22.8 Hz at I_+.

Also plotted in Fig. 7.6 is the steady-state voltage V as a function of the sustained current I_{ss} flowing across the membrane. I_{ss} can be obtained solving for I in Eqs. 7.1 under steady-state conditions. Similar to the steady-state I–V relationship for the squid axon membrane (Fig. 6.9A), this curve is a monotonically increasing function. Operationally, it

can be obtained by injecting a current step of amplitude I into the system and plotting the resulting membrane potential.

7.2 The Morris–Lecar Model

It has been argued that the FitzHugh–Nagumo equations do not faithfully represent any particular neuronal membrane and that phase space analysis therefore is not a particular useful tool to understand the dynamics of "real" neurons. Because we think otherwise, we will apply phase space analysis to a second set of equations, which is meant to capture the dynamics of the membrane potential in the muscle of barnacles. Here all terms can be directly identified with various voltages and conductances. These equations also allow us to demonstrate a very different way in which the onset of oscillations can occur. In the so-called *saddle* bifurcation, oscillations first emerge with an arbitrarily small frequency. As the amplitude of the injected current is smoothly increased, the frequency of the spike trains also increases.

Barnacle muscle fibers that are subject to constant current inputs respond with a variety of oscillatory voltage patterns. In order to describe these, Morris and Lecar (1981) postulated a set of coupled, ordinary differential equations (neglecting any spatial dependencies) incorporating two ionic currents: an outward going, noninactivating potassium current and an inward going, noninactivating calcium current. Because the Ca^{2+} current responds much faster than the K^+ current, we assume that $I_{Ca}(t)$ is always in equilibrium for the time scales we are considering. This allows us to neglect the dynamics of the calcium current and we only need to treat the two-dimensional reduced version of the equations. Different variants of the Morris-Lecar equations are in usage. We will follow the presentation in Rinzel and Ermentrout (1998) which demonstrates best the two distinct manners in which a system can start to oscillate.

7.2.1 Abrupt Onset of Oscillations

In their reduced form, the equations showing this generic type of behavior are

$$\begin{aligned} C_m \frac{dV_m}{dt} &= -I_{\text{ionic}}(V_m, w) + I(t) \\ \frac{dw}{dt} &= \frac{w_\infty(V_m) - w}{\tau_w(V_m)} \end{aligned} \tag{7.11}$$

where V_m is the absolute membrane potential (in millivolts), $C_m = 1\mu\text{F/cm}^2$, w is the activation variable for potassium, all currents are in units of microamperes per square centimeter ($\mu\text{A/cm}^2$) and time t is measured in milliseconds. The ionic current has three components,

$$I_{\text{ionic}}(V_m, w) = \overline{G}_{\text{Ca}} m_\infty(V_m)(V_m - E_{\text{Ca}}) + \overline{G}_{\text{K}} w(V_m - E_{\text{K}}) + G_m(V_m - V_{\text{rest}}) . \tag{7.12}$$

*As stated above, we assume that the calcium current is always at equilibrium, with its activation curve given by

$$m_\infty(V_m) = 0.5\left(1 + \tanh\frac{V_m + 1}{15}\right) . \tag{7.13}$$

The potassium activation variable follows the standard first-order Eq. 6.7 with steady-state activation

$$w_\infty(V_m) = 0.5\left(1 + \tanh\frac{V_m}{30}\right) \tag{7.14}$$

and time constant

$$\tau_w(V_m) = \frac{5}{\cosh V_m/60}. \tag{7.15}$$

The other parameters are $\bar{G}_{Ca} = 1.1$, $\bar{G}_K = 2.0$, $G_m = 0.5$, $E_{Ca} = 100$, $E_K = -70$, and $V_{rest} = -50$ (all conductances are in units of millisiemens per square centimeter and the reversal potentials in millivolts).

Following the methods described in the first part of this chapter, we characterize the phase space associated with these equations by the two nullclines (Fig 7.7A). For the parameters used here, the nullclines intersect at a single location, no matter what the amplitude of the injected current I. We obtain a physiological picture of events in a muscle when we depolarize the membrane by injecting a sustained current $I = 15\ \mu A/cm^2$. Under these conditions, the equilibrium point is stable and the resting membrane potential is -31.7 mV.

Applying current pulses that briefly depolarize the system from its resting state demonstrates the existence of a threshold and a limit cycle. As long as the membrane is depolarized to less than -14.8 mV, the system quickly returns to its resting state (after a brief hyperpolarization; see Fig. 7.7). Depolarizing the membrane past -14.8 mV triggers a stereotypical behavior, following a very similar limit cycle to the one shown by the FitzHugh–Nagumo model. Indeed, different initial conditions (in the case of Fig. 7.7 depolarizing the membrane to either -14.7 or to -12 mV) has little effect on the phase space trajectory (besides speeding up initiation of the spike).

Figure 7.8 summarizes the behavior of the system to constant current steps. Panel 7.8A is a plot of the steady-state membrane potential as a function of the applied current. Following Eqs. 7.11, this is identical to the steady-state ionic current $I_{ionic}(V_m, w_\infty(V_m))$. In this system, the sustained I–V relationship is strictly monotonic. As more and more current is injected, the membrane is depolarized from rest at -31.7 mV (in the presence of the stabilizing 15-$\mu A/cm^2$ current injection), and the w nullcline intersects the V_m nullcline along its middle portion (Fig. 7.7A). Similar to the FitzHugh–Nagumo equations which experience the onset of oscillations via a subcritical Hopf bifurcation, the real part of the two conjugate eigenvalues goes to zero (at $I_- = 24.9\ \mu A/cm^2$) and then becomes positive, indicating loss of stability. At the same time, a stable limit cycle appears: the system generates an infinite train of action potentials. For a limited region of current amplitudes, the equilibrium point remains unstable (as indicated by dashes in Fig. 7.8A) and the system spikes. All of this is more or less identical to what happens in the FitzHugh–Nagumo equations. Let us now change these equations in a minor way to obtain quite a different behavior.

7.2.2 Oscillations with Arbitrarily Small Frequencies

A key property of a Hopf bifurcation is that if the system oscillates, it will oscillate at a well-defined minimum frequency, as the squid axonal membrane and indeed most axons. However, numerous cell types, such as pyramidal cells in cortex, can generate trains of spikes with large interspike intervals, that is, with very low oscillation frequencies upon current injection (see Fig. 9.7; Connor and Stevens, 1971c).

Here, the onset of oscillations is governed by a dynamical mechanism different from the Hopf bifurcation, which can be observed in a slightly modified version of the Morris–Lecar equations. What has to occur is that the nullclines must intersect several times. We

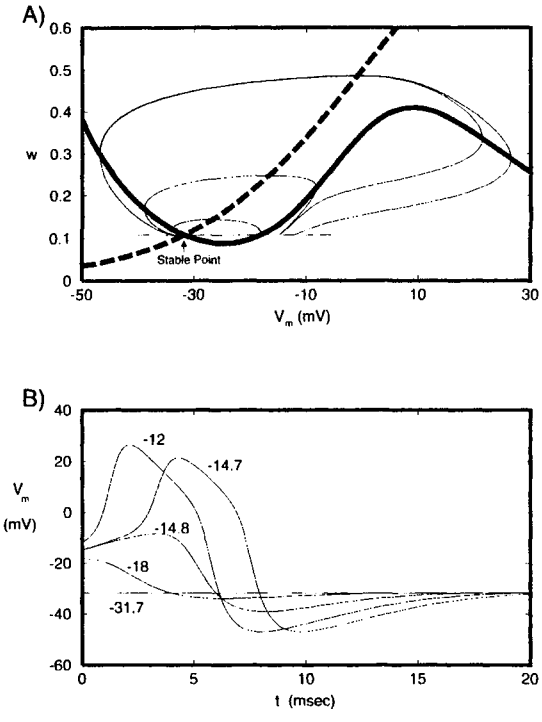

Fig. 7.7 Response of the Morris–Lecar Model to Current Pulses Equations 7.11, describing electrical events in the muscle cells of barnacles (Morris and Lecar, 1981), show a qualitatively similar behavior to the squid axon membrane and to the FitzHugh–Nagumo equations. **(A)** Phase plane portrait (here membrane potential V_m versus potassium activation w) for different stimulus conditions. The nullclines are plotted in bold. In the presence of a stabilizing current injection, the resting potential is -31.7 mV. From this state, the system is stimulated by brief current pulses, instantly depolarizing the membrane (thin lines). If the stimulus depolarizes the muscle to either -18 or to -14.8 mV, the system responds with a subthreshold excursion around the resting potential (two innermost loops around the resting potential). For larger values, the system moves along a limit cycle: it spikes. **(B)** Evolution of the membrane potential V_m for this stimulus paradigm.

can achieve this by assuming, for example, that the potassium activation is a much steeper function of voltage than before. Following Rinzel and Ermentrout (1998), we modify the potassium activation as well as its dynamics,

$$w_\infty(V_m) = 0.5\left(1 + \tanh\frac{V_m - 10}{14.5}\right) \tag{7.16}$$

and

$$\tau_w(V_m) = \frac{3}{\cosh\dfrac{V_m - 10}{29}}. \tag{7.17}$$

We also decrease the amount of calcium conductance by 10% to $\overline{G}_{Ca} = 1$. All other parameters remain unchanged.

As witnessed by Fig. 7.9, this fundamentally changes the character of the phase portrait. Now, three equilibrium points exist. If we were to carry out a linear stability analysis, we would find that the lower point is a stable sink (that is, both eigenvalues are real and negative),

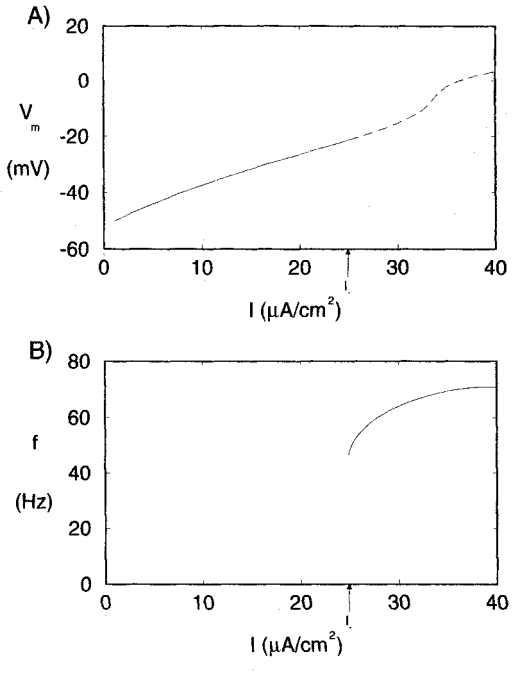

Fig. 7.8 SUSTAINED SPIKING IN THE MORRIS–LECAR MODEL **(A)** Steady-state voltage and **(B)** oscillation frequency as a function of the amplitude of the sustained current I for the reduced Morris–Lecar model (Eqs. 7.11). The steady-state I–V curve can also be viewed as the cumultative, steady-state ionic current flowing at any particular membrane potential V_m. At $I_- = 24.9\ \mu\text{A/cm}^2$ (arrow), the single equilibrium point (Fig. 7.7A) loses stability via hard excitation (a subcritical Hopf bifurcation) when the real part of the two conjugate eigenvalues goes through zero and becomes positive. As in the case for the Hodgkin–Huxley and FitzHugh–Nagumo equations, this type of onset of oscillations implies a nonzero oscillation frequency (here a minimum of 50 Hz).

the middle one is an unstable saddle (one eigenvalue is positive and the other negative), while the upper equilibrium point is an unstable spiral (the eigenvalues are complex, with their real part being positive; Fig. 7.9A). Indeed, the lower resting state at $V_m = -29.2$ mV and $w = 0.0045$ is a globally attracting rest state. A local perturbation in its neighborhood leads to a prompt decay back to rest, while a large input pulse will cause the system to move on its usual trajectory around the phase space, a trajectory that ultimately ends at rest again: the system responds to a brief current pulse with a spike before settling down again. However, different from the previous systems we analyzed, this one shows a true *threshold* due to the presence of the unstable saddle.

The middle equilibrium point, associated with the negative and the positive real eigenvalues, is called a *saddle* because it comes with a curve, called the *separatrix* curve, which sharply distinguishes between sub- and suprathresholds: any phase point to the left of this curve will veer away from equilibrium toward the stable sink, while any point to the right of the separatrix will move in that direction and generate a spike (Fig. 7.9B). If the initial condition places the system near the threshold separatrix, the system will display a long latency before decaying back or spiking, because being close to both nullclines implies that both variables V_m and w change only slowly.

What happens if the amplitude of the injected current is increased? This has the effect of lifting the V_m nullcline closer to the w nullcline and moving the two lower equilibrium points

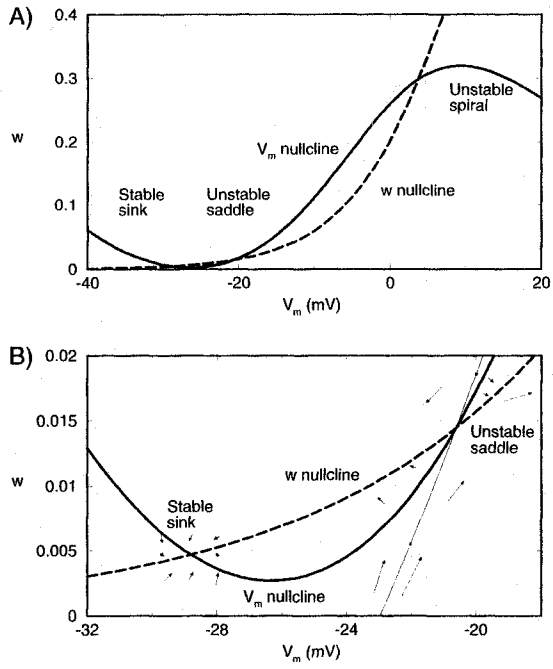

Fig. 7.9 System with Multiple Equilibrium Points The Morris–Lecar equations were modified by changing the dynamics of potassium activation and making its voltage dependency steeper (Eqs. 7.16 and 7.17). **(A)** Under these conditions, the two nullclines can intersect up to three times. Here, the lower equilibrium point is a globally attracting, *stable sink*, the middle one an *unstable saddle*, and the upper one an *unstable spiral*. **(B)** Phase space portrait around the two lower equilibrium points. The separatrix curve (thin line) at the saddle strictly separates sub- and suprathreshold regions of phase space. Points to the left of this curve will decay back to the stable sink, while points to the right will lead to a spike. If the current injected into the system is further increased, these two equilibrium points will move toward each other, coalesce, and disappear. If the initial state of the system lies in the neighborhood of these two curves, it will evolve very slowly since, by definition, $\dot{V}_m = 0$ along the V_m nullcline and $\dot{w} = 0$ along the w nullcline, explaining why the system is able to spike at very low frequencies.

closer and closer to each other. For a critical value $I_1 = 8.326\ \mu\text{A/cm}^2$, the stable sink and the unstable saddle meet and coalesce and—upon further increases of I— disappear entirely. A *saddle-node bifurcation* has just occurred (Rinzel and Ermentrout, 1998), with the system losing two of its equilibrium points. At the point when the two critical points meet, the two eigenvalues are identical to zero.

If the state of the system is in the neighborhood of these two points (as in Fig. 7.9B), it will take a long time to move into a different region of phase space. (After all, by definition, the change in one or the other variable along the nullclines is zero.) Indeed, the closer the system is to the nullclines, the slower it will move. At I_1, that is, when the two equilibrium points have coalesced, the period of the oscillations is infinite. It can be shown under some fairly generic conditions (Strogatz, 1994) that the oscillation frequency is proportional to $\sqrt{I - I_1}$ (Figs. 7.10 and 7.11B).

A property of systems with a saddle-node bifurcation is an N-shaped relationship between the membrane potential and the injected current, or between the potential and the sustained current (Fig. 7.11A). In other words, for a range of membrane currents three different steady

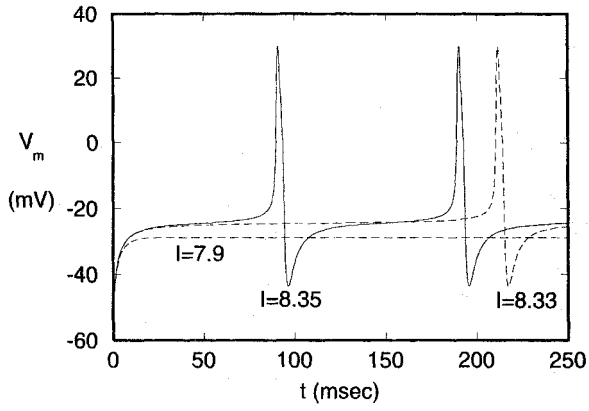

Fig. 7.10 SPIKING AT LOW FREQUENCIES Response of the modified Morris–Lecar equations (Eqs. 7.16 and 7.17) using current steps (starting at $t = 0$) of variable amplitude. In response to a current step of 7.9 μA/cm^2 amplitude, the membrane depolarizes. Close to $I_1 = 8.326$ μA/cm^2, the onset of spiking can be delayed almost indefinitely, similar to the delay observed in pyramidal cells due to the presence of the A-like current (Fig. 9.7). This is not caused by the very slow time constant of any one ionic current, but it is due to the structure of the nullclines in phase space (Fig. 7.9B).

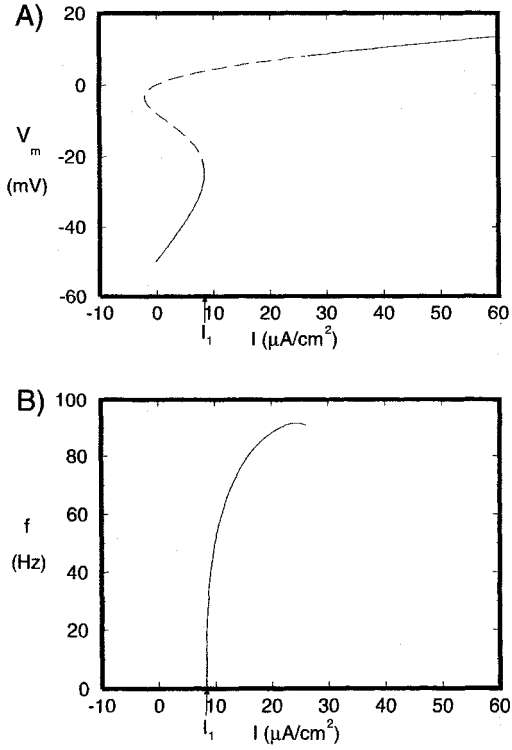

Fig. 7.11 SUSTAINED SPIKING IN THE MODIFIED MORRIS–LECAR MODEL (A) Steady-state voltage and **(B)** oscillation frequency as a function of I for the modified Morris–Lecar model (Eqs. 7.16 and 7.17). Different from Fig. 7.8, the I–V relationship is N-shaped. Spiking first occurs at I_1 (arrow) when the slope of this curve is infinite and then becomes negative. This happens when the two lower equilibrium points in the phase portrait of Fig. 7.9 merge, creating oscillations with arbitrarily long interspike intervals via a saddle-node bifurcation.

state voltages exist, of which only one, however, is stable (solid portion of the curve). When the injected current is slowly increased, oscillations first occur when the slope of the I–V curve becomes infinite (for $I = I_1$) and then negative. If very large stimulus currents are used, the system locks up at very depolarized levels and spiking ceases.

In this model, the transition from a stable equilibrium point to a stable limit cycle is marked by arbitrarily low firing rates *without* having to rely on arbitrarily slow activation rates. Having a saddle is a necessary condition for such a continuous f–I relationship. In our case, this is achieved via a steep nonlinear relationship between the membrane potential and activation of the potassium conductance. As we will see in Chap. 9, this is the characteristic action of a transient potassium current (the I_A current of Connor and Stevens, 1971c), which has a steep voltage dependency in the neighborhood of the resting state of the cell.

7.3 More Elaborate Phase Space Models

So far, we reviewed models of spiking that are constrained to a two-dimensional phase space. However, a variety of higher dimensional models have been studied to characterize more complex behavior, in particular *bursting* and intrinsic rhythmic behavior.

Thalamic cells can respond to input by either firing a few fast action potentials or generating a slow calcium, all-or-none event, on top of which ride a series of fast, conventional sodium spikes. Which response type occurs depends on the level of membrane depolarization (Jahnsen and Llinás, 1984a,b; Fig. 9.4). Researchers have generated detailed biophysical models of the various ionic currents that are responsible for this behavior (McCormick and Huguenard, 1992). Given the potential significance of bursting as a special means of communicating a privileged symbol, we dedicated Chap. 16 to this topic.

Rose and Hindmarsh (1985) use phase space models with three variables: one for the membrane potential, one for the degree of accommodation, and one to mimic slow adaptation. They proved that it is this slow variable that is responsible for determining whether the neuron fires in a tonic or in a burst mode in response to sustained current input. Indeed, a classification of bursting based on this type of phase-space analysis is beginning to emerge (Wang and Rinzel, 1995).

As reviewed extensively by Llinás (1988), many neurons do not behave at all like the squid axon membrane, but have a great deal of diversity of electrical behaviors. For instance, subsets of thalamic cells express complex intrinsic oscillations of the membrane potential in very different frequency bands (from a few to 40 Hz or more) depending on the behavioral state of the animal (sleep, arousal, etc.; see Steriade, McCormick, and Sejnowski, 1993). In order to understand the interplay between intrinsic cellular properties and network properties that generate these period phenomena, networks of thalamic cells with more than half a dozen ionic conductances have been simulated (Destexhe, McCormick, and Sejnowski, 1993; Wang, 1994; Contreras et al., 1997). Although the underlying phase spaces are high-dimensional, their projection onto suitable two-dimensional subspaces has shown the usefulness of analyzing the behavior of these systems in terms of the concepts introduced in this chapter.

7.4 Recapitulation

The theory of nonlinear dynamics represents a powerful tool to characterize the generic mechanisms giving rise to the threshold response, the stereotypical shape of action potentials, or the onset of oscillations. It allows us to understand why these phenomena occur even when we have insufficient information concerning the detailed kinetics or the exact shape of the various rate and time constants. In this chapter, we apply the theory of dynamical systems

to analyze two-dimensional systems with the help of the phase portrait. In particular, we focus on the FitzHugh–Nagumo (FitzHugh, 1961, 1969; Nagumo, Arimoto, and Yoshizawa, 1962) and the Morris–Lecar (1981) models of spiking.

The FitzHugh–Nagumo model was based on the observation that the membrane potential and the sodium activation in the four-dimensional Hodgkin–Huxley equations evolve on a similar time scale, while the sodium inactivation and the potassium activation also share similar behavior, albeit on a slower scale. This feature can be exploited by expressing the membrane excitability via the two-dimensional FitzHugh–Nagumo equations with constant coefficients, with V corresponding to the excitability of the system and W its degree of accommodation. Linear stability analysis allows us to understand why the resting state is stable and when spiking first occurs. It is also helpful to explain the all-or-none shape of the action potential as an example of a limit cycle, upon which the system will rapidly converge once threshold is exceeded.

We also acquainted the reader with a qualitativly similar system of equations that describes muscle fiber excitability in terms of a leak, a calcium, and a potassium current (Morris and Lecar, 1981). Following the lead of Rinzel and Ermentrout (1998), we assume that the calcium current is so rapid that it is always in the steady-state with respect to the membrane potential and the potassium activation, and we discuss two variants of these equations. The first behaves similar to the squid axon and to the FitzHugh–Nagumo equations, generating oscillations with a nonzero oscillation frequency (via a subcritical Hopf bifurcation). Modifying the potassium conductance to be a steeper function of V_m allows the system to spike at very low frequencies via a saddle-node bifurcation, similar to what occurs in cells that have a marked delay between the onset of current injection and the first spike (due to the presence of I_A).

The advantage of using models based on a very small number of variables—rather than relying on biophysical very detailed models with an exuberance of variables—is that they offer us a qualitative, geometrical way to understand why a cell spikes and why it switches between two modes of firing without necessarily having to know every single detail of the system.

Given the enormous numerical load involved in simulating the dynamics of hundreds or thousands of neurons, such a simplified single-cell model will allow us to study neural networks containing realistic numbers of neurons. The price one pays for this reduced complexity is a lack of quantitative predictions.